Stopping of Havar, nickel, Kapton, and Mylar for 5–19-MeV ^{16}O ions

J. Räisänen and E. Rauhala

Accelerator Laboratory, University of Helsinki, Hämeentie 100, SF-00550 Helsinki 55, Finland

In order to determine stopping-power values the energy losses of 5.2–22.5-MeV ^{16}O^{n+} ions in 2.0-μm Havar, 2.8-μm nickel, 10.5-μm Kapton, and 3.8- and 6.9-μm aluminum-layered (40-nm Al) Mylar foils were measured in transmission geometry. Proton energy loss in a backscattering experiment was taken as a measure of film thickness. The measured stopping-power and energy-loss data were compared with calculated predictions obtained by using Bragg's additivity rule and the Andersen-Ziegler parameters for proton stopping with appropriate scaling for oxygen ions and with experimental values available in the literature. The results for the foils of medium atomic number, Havar and nickel, were found to be similar to calculated values; however, the experimental stopping powers lie 2–4% above the predicted values between 6 and 14 MeV for the light composite Mylar and Kapton foils. The response of silicon surface-barrier detectors to ^{16}O ions was studied in the energy interval 1.5–19 MeV. A distinct nonlinearity was observed at low ion energies.

INTRODUCTION

The knowledge of accurate energy-loss and stopping-power values for various foil materials has significant practical importance in experimental work with heavy ions. The results also give valuable information for comparisons with theory.

No previous experimental data have been given in the literature for oxygen ions in Havar and Kapton foils. Only the energy-loss data given by Schambra *et al.*[1] may be found for Mylar. Some stopping-power data exist[2–4] for nickel which may be used for comparisons. In the present work we have continued the systematic determination[5–7] of accurate experimental stopping-power and energy-loss data for energetic ions with measurements of ^{16}O ions in 2.0-μm Havar, 2.8-μm nickel, 10.5-μm Kapton, and 3.8-μm and 6.9-μm Mylar foils. The possible nonlinear response of the silicon detector to heavy ions has been measured and taken into account in calculating the experimental values.

EXPERIMENT

The ion beams were generated by the 5-MV EGP-10-II tandem accelerator (^{16}O) and the 2.5 MV Van de Graaff accelerator (^{1}H) of the University of Helsinki. The charge of the oxygen-ion beam was 2 + for energies between 6 and 11 MeV, 3 + for energies between 11 and 16 MeV, 4 + for energies between 17 and 23 MeV, and 5 + for energies above 16 MeV. The energies and charge states overlap as the charge state effects on the stopping of the oxygen ions was being investigated.

The experimental arrangement is described in detail in Ref. 5. Energy losses were measured in transmission geometry by interposing the sample foils into the scattered ion beam from a thick gold target. The most probable energy loss of the ions in the foil was then determined by observing the shift of the backscattering signal,

induced by the foil. The silicon surface-barrier detector (50 mm^2 area, 100 μm sensitive depth) was positioned at a scattering angle θ which was 150°. The detector solid angle was 4 mSr. In this way a low intensity ion flux was provided and direct beam exposure of the foils was avoided. Only the metallic foils of Havar and nickel could be exposed to the direct beam.[5,6] For comparison purposes a few data points were measured by placing the Havar and nickel foils in the direct beam. The energy resolution of the detection system was 150 keV at $E_0 = 17.0$ MeV.

The areal densities of the foils were measured subsequent to the energy-loss experiments by proton backscattering using standard backscattering apparatus. Details of the composite foil materials are given in Table I.

MEASUREMENTS AND RESULTS

Recently we have demonstrated[5] that the nominal compositions, Bragg's additivity rule, and semiempirical proton stopping in elemental matter by Andersen and Ziegler[8] can be used to accurately predict the stopping of 1–2.4 MeV protons in the composite materials studied in this work. Therefore the direct measurement of the local areal density $N \Delta x$ (N atomic density, Δx foil thickness) by proton backscattering yields more accurate thicknesses and stopping powers than other methods of thickness measurement (e.g., weighing). In this work 2.2-MeV proton backscattering was thus employed at the exact position of the heavy ion beam on the foil. To convert the areal density to thickness nominal mass densities of 8.30, 8.91, 1.42, and 1.39 for Havar, nickel, Kapton, and Mylar, respectively, were used. An accuracy of 2% is estimated for the resulting thickness values of the foils given in Table II.

When ions of different energy are absorbed in Si detector material the energy response of the detector is affected by the surface dead layer and nonionizing pro-

TABLE I. Nominal compositions, average atomic weights, and specific gravities of Havar, Kapton, and Mylar foils.

Foil	Element	Concentration (at. %)
Havar ($M =57.6$ amu, $\rho=8.30$ g/cm^3)	Be	0.3
	C	1.0
	Cr	22.2
	Mn	1.7
	Fe	18.1
	Co	41.6
	Ni	12.8
	Mo	1.4
	W	0.9
Kapton $(C_{22}H_{18}O_5N_2)_x$ ($M =9.63$ amu, $\rho=1.42$ g/cm^3)	H	38.3
	C	46.8
	N	4.3
	O	10.6
Mylar $(C_{10}H_8O_4)_x$ ($M =8.73$ amu, $\rho=1.39$ g/cm^3)	H	36
	C	45
	O	18

cesses.[9] One consequence of this is that the particle energy per channel is not constant. A nonlinearity of $\sim 5\%$ in alpha particle energy per channel has been observed below 0.6 MeV.[10,11] This effect was checked to determine if it interferes with the present stopping-power measurements. At different detected ^{16}O ion energies E_1 the detected energy differences ΔE_1 of the backscattering gold signals were divided by corresponding channel intervals Δchannel. The result is illustrated in Fig. 1.

The horizontal bars give the magnitudes of the energy differences and the vertical bars indicate the experimental error due to uncertainties in signal positions. A linear, almost constant energy dependence of particle energy per channel on energy above 4 MeV is observed. Below 4 MeV $\Delta E_1/\Delta$channel rapidly increases, being 10% higher at 1.5 MeV than at 4 MeV. A titanium target was used below $E_1=7$ MeV to scatter the oxygen ions, below 3 MeV an aluminum one was employed.

TABLE II. The energy loss ΔE of 5.17–23.00 MeV ^{16}O ions in Havar, nickel, Kapton, and Mylar foils.

E (MeV)	ΔE (MeV) in				
	Havar (2.01 μm)	nickel (2.76 μm)	Kapton (10.51 μm)	Mylar (3.77 μm)	Mylar (6.88 μm)
23.00	7.65±0.10	11.75±0.10			
20.66	8.17±0.10	12.16±0.10	12.64±0.10	4.57±0.10	8.86±0.10
19.19	8.41±0.10	12.32±0.10	13.24±0.10	4.78±0.10	9.25±0.10
17.71	8.57±0.10	12.38±0.10	13.74±0.15	4.94±0.10	9.54±0.10
16.97	8.61±0.10	12.35±0.15	13.90±0.15	5.02±0.10	9.74±0.10
16.24	8.55±0.10	12.34±0.15	14.11±0.20	5.10±0.10	9.97±0.15
15.50	8.59±0.10	12.21±0.20	14.13±0.25	5.16±0.10	10.11±0.15
14.76	8.61±0.10	12.06±0.20	13.96±0.30	5.23±0.10	10.22±0.20
14.02	8.63±0.15	11.91±0.25	13.60±0.30	5.31±0.15	10.48±0.20
13.28	8.61±0.15	11.73±0.25	13.10±0.30	5.43±0.15	10.51±0.25
12.55	8.57±0.15	11.27±0.30		5.33±0.15	10.57±0.25
11.81	8.53±0.15	10.91±0.30		5.62±0.15	10.43±0.30
11.07	8.35±0.20	10.46±0.30		5.73±0.15	10.18±0.30
10.33	8.17±0.20			5.83±0.15	9.82±0.30
9.59	7.91±0.25			5.80±0.20	
8.86	7.63±0.25			5.85±0.20	
8.12	7.26±0.30			5.86±0.25	
7.38	6.71±0.30			5.71±0.25	
6.64	6.21±0.30			5.53±0.30	
5.90				5.27±0.30	
5.17				4.57±0.30	
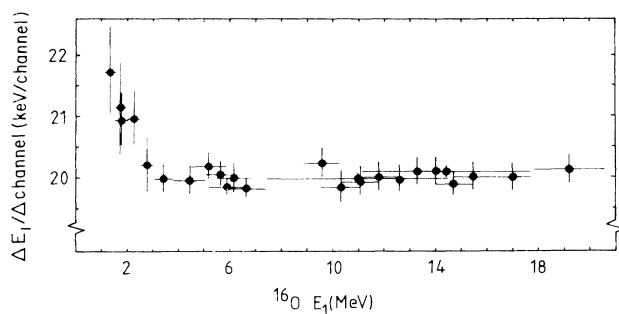
FIG. 1. Particle energy per channel for ^{16}O ions as a function of ion energy incident on a standard surface barrier (50 mm^2, 100 μm) Si detector.

FIG. 2. The stopping powers of ^{16}O ions in Havar, nickel, Kapton, and Mylar as a function of corrected mean ion energy (see text). The dashed curves are calculated by assuming Bragg's additivity rule, proton stopping (Ref. 8), and scaling (Ref. 16) for oxygen ions. The solid lines were fitted to the experimental data to guide the eye.

The magnitude of this effect is in excellent agreement with the values of Lennard et al.[10] obtained in the energy region 0.7–2.5 MeV. The effect on the present energy-loss data has been corrected where it is significant, i.e., for a few data points at the low end of the energy range for each of the foils.

The stopping powers of the foil materials are summarized in Table III. The stopping $S = dE/dx$ (differential energy loss per unit path length) is taken as $\Delta E/\Delta x$ (ΔE is the energy loss in the foil of thickness Δx) at an effective energy E. To obtain E a small correction to the mean ion energy $E_{av} = E_i - \Delta E/2$ (E_i = incident energy) in the foil has been applied to allow for the nonlinear energy dependence of the stopping values. In this way ac-

curate stopping powers from the ion energy losses ΔE may be extracted when $\Delta E < E_{av}$.[12] This condition, however, is not fulfilled for the lower energy range of the present energy loss measurements. Therefore, to include all our experimental data, the energy loss values are also given in Table II.

TABLE III. The stopping-power values of ^{16}O ions for Mylar, Havar, nickel, and Kapton.

E (MeV)	Mylar	E (MeV)	Havar	E (MeV)	nickel	E (MeV)	Kapton
				Stopping power (MeV cm^2/mg)			
18.35	8.72[a]	19.06	4.59	16.84	4.78	14.04	8.47
16.76	9.12[a]	16.43	4.90	14.23	4.95	12.20	8.87
16.09	9.26[b]	14.82	5.04	12.63	5.02		
15.19	9.43[a]	13.23	5.14				
14.41	9.67[b]	12.45	5.16				
14.40	9.58[a]	11.75	5.12				
13.64	9.73[a]	10.97	5.15				
12.88	9.84[a]	10.20	5.16				
12.74	9.97[b]	9.43	5.17				
12.08	9.98[a]	8.68	5.16				
11.87	10.17[b]	7.95	5.14				
11.30	10.13[a]						
11.00	10.43[b]						
10.50	10.36[a]						
10.11	10.57[b]						
9.67	10.55[a]						
9.24	10.69[b]						
8.87	10.72[a]						
8.06	10.93[a]						
7.25	11.13[a]						
6.50	11.07[a]						
5.72	11.16[a]						
4.94	11.18[a]						

[a]From 3.77 μm foil data.
[b]From 6.88 μm foil data.
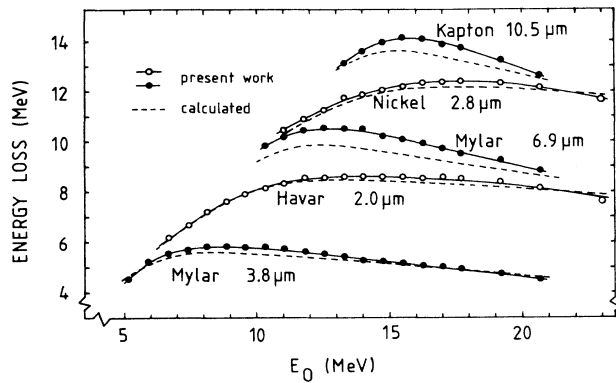
FIG. 3. Energy-loss data of ^{16}O ions in the foils of Table II as a function of incident ion energy. The dashed and solid curves as in Fig. 2.

FIG. 4. Present stopping powers of Ni compared with earlier literature values[2-4] and the calculated dashed curve (as in Fig. 2).

The uncertainties of the data given in the tables are estimated from the possible experimental errors in determining signal positions in the ^{16}O energy loss and ^{1}H backscattering experiments, and the inaccuracy of the thicknesses of the foils.

DISCUSSION

To extend the energy interval covered and to further confirm our data the energy loss of the ions at maximum available energy was also determined by placing the metal foils in a direct beam. The detector in this setup was positioned at a 30° forward-scattering angle. The stopping values at 19.1 MeV (Havar) and 16.8 MeV (nickel), and the energy-loss values at 23 MeV were thus obtained by an independent experimental method in the transmission geometry.

All our stopping and energy-loss values may be fitted by slowly varying curves within the error limits. The internal consistency of our results is thus verified. Stopping powers obtained from Mylar foils of different thickness are in good agreement, thus no dependence on target thickness[13] at high ^{16}O-ion velocities $(5-8)v_0$ ($v_0 = $ Bohr velocity) could be detected.

No evidence of a dependence on the charge state of the ion beam from the accelerator could be detected within experimental accuracy. The possibility of charge changing effects[14,15] is still not ruled out, since an equilibrium independent of the initial charge is probably attained[15] after scattering from the gold target.

The results are compared in Figs. 2 and 3 with the calculated stopping and energy loss obtained using Bragg's additivity rule and the Ziegler scaling[16] of proton stopping for the heavy-ion stopping cross sections. The present experimental ^{16}O-ion stopping powers in Mylar agree well with the calculated curves at the
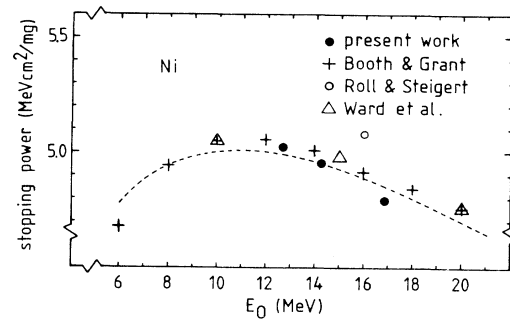
higher energies but increasingly exceed the calculated predictions as the energy decreases. The difference is 4–2% between 6 and 12 MeV. The same trend is observed in our stopping data for Kapton and evident from the Kapton energy-loss values. For both Havar and nickel a good consistency between experimental and predicted stopping and energy loss was observed over the entire energy range.

The energy-loss results of Fig. 3 are in good agreement with calculations for all the foils in the lower end of our energy interval. These energies fall below the maximum of the stopping-power curve in each case. The maxima in our energy-loss curves appear to be shifted by 2–3 MeV towards higher energies than in the calculations.

As far as we know there are no previous values for ^{16}O ions in Havar and Kapton in the literature. One reference[1] for ^{16}O-ion stopping in Mylar can be found. In this case, however, accurate comparison with our results cannot be made because exact data of the common energy interval are not given in this study.

Comparisons of our Ni stopping powers with existing experimental data[2-4] and their relation to the calculations are presented in Fig. 4. All the data (excluding that[3] at 16 MeV) agree within 2%. The maximum deviations from the calculated dashed curve are only 1%.

In conclusion, the present results obtained in transmission geometry indicate 2–4 % higher ^{16}O-ion stopping in our intermediate energy region 6–14 MeV for the light composite foils Mylar and Kapton than the scaled semi-empirical proton stopping used in conjunction with Bragg's additivity rule. There is good agreement for the heavier metallic Havar and nickel foils. In the case of nickel, which had been experimented on before, our results are consistent with the previous data. A distinct nonlinearity in the energy response of a silicon surface barrier detector to ^{16}O ions below 3 MeV has been observed.

[1]P. E. Schambra, A. M. Rauth, and L. C. Northcliffe, Phys. Rev. 120, 1758 (1960).
[2]W. Booth and I. S. Grant, Nucl. Phys. 63, 481 (1965).
[3]P. G. Roll and F. E. Steigert, Nucl. Phys. 17, 54 (1960).

[4]D. Ward, R. L. Graham, and J. S. Geiger, Can. J. Phys. 50, 2302 (1972).
[5]E. Rauhala and J. Räisänen, Nucl. Instrum. Methods B 12, 321 (1985).

[6]J. Räisänen and E. Rauhala, Phys. Rev. B **35**, 1426 (1987).

[7]E. Rauhala and J. Räisänen, Nucl. Instrum. Methods B **24**, 362 (1987).

[8]H. H. Andersen and J. F. Ziegler, *Hydrogen Stopping Powers and Ranges in All Elements* (Pergamon, New York, 1977).

[9]W. N. Lennard and K. B. Winterbon, Nucl. Instrum. Methods B **24/25**, 1035 (1987).

[10]W. N. Lennard, H. Geissel, K. B. Winterbon, D. Phillips, T. K. Alexander, and J. S. Forster, Nucl. Instrum. Methods A **248**, 454 (1986).

[11]E. Rauhala, J. Appl. Phys. **62**, 2140 (1987).

[12]D. I. Porat and K. Ramavataram, Proc. R. Soc. London, Ser. A **252**, 394 (1959).

[13]W. N. Lennard, D. Phillips, I. V. Mitchell, H. R. Andrews, and D. Ward, Nucl. Instrum. Methods B **2**, 153 (1984).

[14]N. E. B. Cowern, P. M. Read, C. J. Sofield, L. B. Bridwell, G. Huxtable, M. Miller, and M. W. Lucas, Nucl. Instrum. Methods B **2**, 112 (1984).

[15]V. P. Zaikov, E. A. Kralkina, V. S. Nikolaev, Yu. A. Fainberg, and N. F. Vorobiev, Nucl. Instrum. Methods B **17**, 97 (1986).

[16]J. F. Ziegler, Appl. Phys. Lett. **31**, 544 (1977).